Conductive graphene as passive saturable absorber with high instantaneous peak power and pulse energy in Q-switched regime

Siti Nur Fatin Zuikafly [a], Ali Khalifa [b], Fauzan Ahmad [a], Suhaidi Shafie [b,*], SulaimanWadi Harun [c]

[a] Malaysia-Japan Institute of Technology, Universiti Teknologi Malaysia, 54100 Kuala Lumpur, Malaysia
[b] Institute of Advanced Technology and Department of Electrical and Electronic Engineering, Faculty of Engineering, Universiti Putra Malaysia, 43400 UPM Serdang, Selangor, Malaysia
[c] Department of Electrical Engineering, Faculty of Engineering, University of Malaya, 50603 Kuala Lumpur, Malaysia

ARTICLE INFO

ABSTRACT

The Q-switched pulse regime is demonstrated by integrating conductive graphene as passive saturable absorber producing relatively high instantaneous peak power and pulse energy. The fabricated conductive graphene is investigated using Raman spectroscopy. The single wavelength Q-switching operates at 1558.28 nm at maximum input pump power of 151.47 mW. As the pump power is increased from threshold power of 51.6 mW to 151.47 mW, the pulse train repetition rate increases proportionally from 47.94 kHz to 67.8 kHz while the pulse width is reduced from 9.58 μs to 6.02 μs. The generated stable pulse produced maximum peak power and pulse energy of 32 mW and 206 nJ, respectively. The first beat node of the measured signal-to-noise ratio is about 62 dB indicating high pulse stability.

Introduction

Q-switching operations can be realized by either active or passive approach. The passively Q-switched technique is rather preferred by researchers as it offers simplicity and flexibility [1] in terms of cavity design. Passively Q-switching does not require external component to modulate its intracavity loss, instead, saturable absorbers (SA) is used to accommodate the function. Various starting material such as graphene, graphite, carbon nanotubes, and topological insulators (TI) [2] have been adapted and investigated as SAs and researchers is still searching for the ideal SA as yet. Saturable absorber based on graphene nano-particles is investigated to obtain evanescent-wave mode-locking regime at which is proven to be a better integration method of the graphene SA as compared to traditional technique which often involves the SA being sandwiched between two fiber ends. The technique yields an improved light transmittance as well as higher modulation depth [3]. Similarly, the SA integration method was also done differently by Lin et al. [4] whom directly imprinted graphite nano-particles on a thinly scribed polyvinyl alcohol (PVA) on a fiber end. This method was claimed to improve the mode-locking performance of the laser by reducing the loss normally induced by the SA's thickness. Single walled carbon nanotubes was investigated as SA with different concentrations and thickness in generating mode-locked laser where it is found that certain level of

concentration and thickness can be varied to be applied for better performance in certain applications [5]. Bismuth (II) Telluride (Bi_2Te_3) topological insulator has also been widely used as SA. A sub-picosecond pulse width of 403 fs was successfully obtained through soliton compression [6].

When first discovered in 2004, graphene is directed towards electronic applications due its excellent electronic properties, but it is further utilized in optical fibres not long after, for its intrinsic optical properties. Graphene consisted of a single atomic layer of sp^2 hybridized carbon atoms arranged in a honeycomb structure [7] and is known for their ultrahigh carrier mobility, thermal conductivity and mechanical strength. Graphene is made commercially available due to the convenience of printing and mass production of said material. A research by Secor et al. [8] on the inkjet printing of conductive graphene shows that the end product demonstrated uniform morphology, compatible with flexible substrate and bending stresses tolerance. Conductive graphene among many other derivatives of graphene, have been put use to many applications involving antennas [9–12] and other electronic devices, such as demonstrated by Dragoman et al. [9], Sayeed et al. [10] and Akbari et al. [11]. Dragoman makes use of the graphene resistivity to control the antenna gain by tuning the graphene's gate voltage while Sayeed fabricated a flexible graphene-based antenna to overcome the drawbacks of commonly used conductor, copper. Another research is also based on conductive graphene antennae for wearable electronics, indicating graphene as mechanically stable material. The advantages offered by conductive graphene is owed to graphene's own stable

---

* Corresponding author.
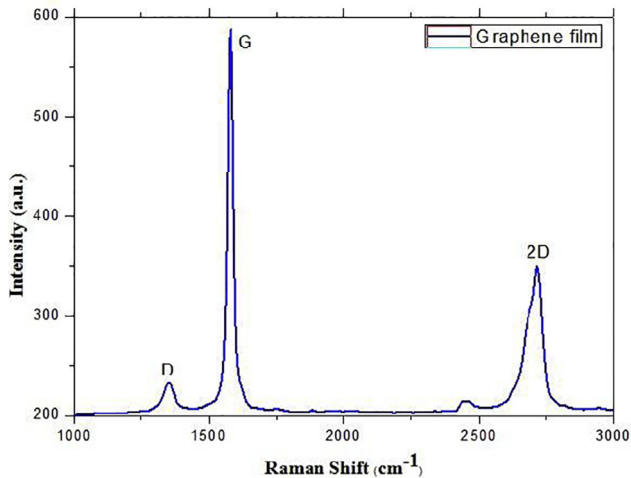   *E-mail address:* suhaidi@upm.edu.my (S. Shafie).

Fig. 1. Raman spectra of graphene film.

mono-atomic structure [13,14]. In the field of fiber lasers and photonics, graphene has been best shown to demonstrate excellent optical properties [15] including ultrawide spectral range due to the linear dispersion of Dirac electrons [1], gapless energy band gap [16], broadband saturable absorption, and ultrafast recovery time among others which allows for ultrashort pulse generation. These optical properties in graphene are used and exploited as saturable absorbers in optical fibres in order to come up with various ranges of practical applications. This work demonstrated the alternative use of conductive graphene as saturable absorber in pulse laser generation, showing ample performance and stability.

To date, numerous works have been reported on the utilization of graphene and its derivatives in pulse laser generation. Graphene oxide (GO) based SA is reported to generate maximum peak power of 16.6 mW [17]. Sobon et al. [18] reported the use of reduced graphene oxide producing a maximum of 125 nJ pulse energy. Besides, in Q-switched regime, graphene SA have also been demonstrated by exfoliating graphene flakes, generating 40 nJ maximum pulse energy [19]. Bogulawski et al. [20] demonstrated the effect of varying layer of GO paper on the laser performance where the highest pulse energy is reported at 36.5 pJ. Monolayer graphene as SA is also demonstrated achieving maximum pulse energy of 2.75 nJ. We demonstrated the generation of Q-switched pulse with 32

mW of instantaneous peak power and 206 nJ of pulse energy by integrating a droplet of conductive graphene solution in Erbium doped fiber laser in ring cavity.

Material preparation and characterization

The Graphene solution was prepared by diluting 15 ml of the commercial ultra-high concentration graphene dispersion (23 wt% graphene) in 5 ml n-Butyl acetate solvent. Then 1.5 ml of ethyl cellulose collide is added to the dispersion as binding material to increase its adhesion to the substrate. Subsequently, the combination was ultrasonicated for 30 min and then stirred for 24 h. The graphene thin layer can be prepared in few method namely drop casting, spin coating and spray methods. In order to study the defects or disorder in the material and to quantify the number of layers of the graphene samples, the prepared graphene samples were characterized using Raman spectrometer (WiTec Alpha 300R) with excitation wavelength of 532 nm at room temperature.

Fig. 1 shows Raman spectra of the graphene film. The spectra; the sharp peaks which reflects the film's crystallinity. The spectra shows three intense features D, G, and 2D bands along the spectra at almost 1351 cm^{-1}, 1578 cm^{-1} and 2712 cm^{-1}, respectively [1]. The D band indicates phonon scattering at defected sites and impurities in sp^2 bonds which are obviously negligible as seen in the spectrum. The long G band is attributed to sp^2 phonon vibrations [2]. The 2D band is found at the higher wavelength in the spectra and doesn't represent defection. However, it confirms the presence of graphene and it originates from a double resonance process that links phonons to the electronic band structure [7]. The shapes of (G) and (2D) bands indicate that the used graphene is multilayer graphene flakes. The calculated intensities ratio I_{2D}/I_G was 0.6; this ratio, together with the low intensity of the D band and the sharp symmetric 2D band are often used to confirm the low defects in the graphene samples.

Graphene samples were also drop casted on glass substrates to measure its electrical conductivity using the four-point probe. Since the generated films are not completely uniform, the measurements were done at different random sites on each sample and then calculating the average value. Fig. 2, describes the influence of the sheet resistance (Rs) by the film thickness.

The results shows that the graphene films present good electrical conductivity. However, the variation in sheet resistance might be due to presence of minor defects. Fig. 2, describes how the sheet resistance decreases as increasing coated film thickness where it was significantly decreased from about 26 $\Omega/\square$ at 5.7 μm to
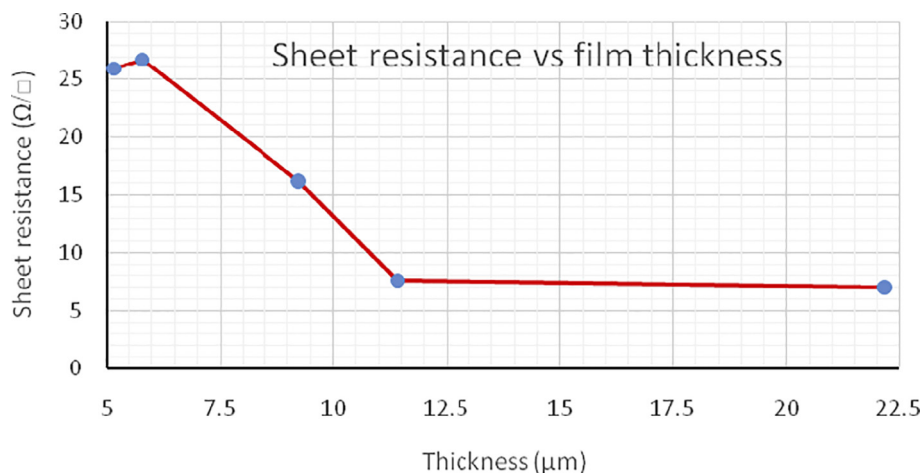

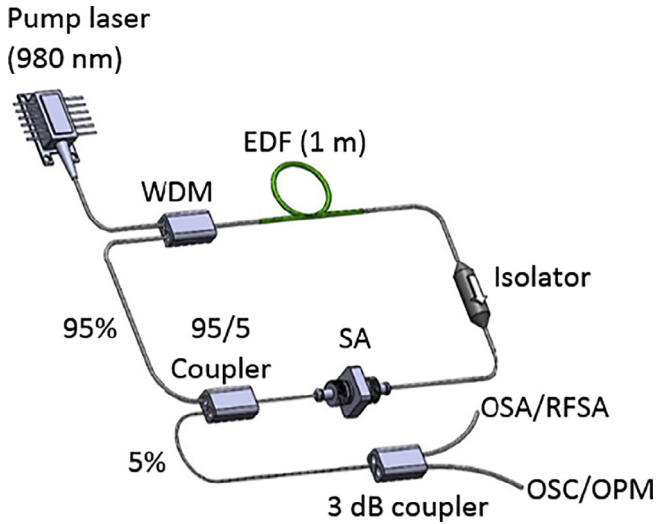**Fig. 2.** Influence of the sheet resistance by the thickness of the graphene films.

Fig. 3. Experimental Setup for Ultrafast Laser Generation Incorporating Conductive Graphene based Saturable Absorber.
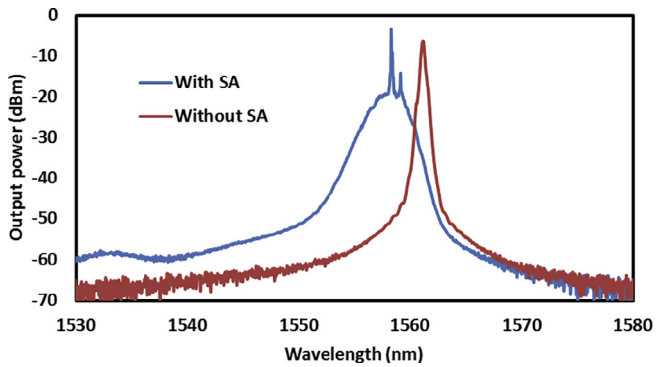

Fig. 4. OSA trace without SA and with SA.

almost 7 $\Omega/\square$ at 11.4 μm. however, the sheet resistance remains steady within 11 μm to 22 μm thick.

Experimental set-up

The experimental setup of the Q-switched laser is as shown in Fig. 3. The newly fabricated diluted graphene is dropped on one end of a fiber ferrule and let dry before integrated in the laser cavity by mating it with another ferrule using a connector. A 1 m long Erbium-doped fiber (EDF) was used as the gain medium. The setup also consist of a 980/1550 nm wavelength division multiplexer (WDM), an isolator, the newly fabricated graphene as SA, and a 95/5 output coupler, arranged in a ring configuration. The core and cladding diameter of the EDF is 8 μm and 125 μm respectively. The numerical aperture of the EDF is 0.16 and has Erbium ion absorptions of 45 dB/m at 1480 nm and 80 dB/m at 1530 nm. The EDF was pumped by a 980 nm laser diode via the WDM. The use of an isolator ensures unidirectional propagation of the oscillating laser. The output of the laser was tapped from the cavity through a 95/5 coupler while keeping 95% of the light to oscillate in the ring cavity. The spectrum of the EDFL was inspected by using the optical spectrum analyzer (OSA) with a spectral resolution of 0.05 nm, whereas the oscilloscope was used to observe the output pulse train via a 460 kHz bandwidth photo-detector.

Experimental results

The laser started to operate in Q-switched regime at 51.6 mW threshold. The optical spectrum of the laser before and after the SA integration is shown in Fig. 4, recorded at maximum possible input pump power of 151.47 mW. The Q-switched laser oscillated at around 1558.28 nm with SA integration compared to 1561.13 nm without the SA. The shifted of the central operating wavelength is due to loss induced by conductive graphene based SA. Carbon based materials such as Graphene is known for having high non saturable losses and low modulation depth [21]. An adequate level of modulation depth is required to achieve a securely stable Q-switching operation as well as to suppress the oscillations of parasitic continuous wave that can be seen as a sharp peak in Fig. 4. This spectral peak can be suppressed by increasing the modulation depth of the SA. The spectral peak formation can also be caused by the reflection of light interference between the optical connectors in the laser cavity [22]. An addition of a polarization controller (PC) in the laser cavity can help in inhibiting parasitic lasing due to the losses in the cavity, thus optimizing the spectrum shape of the pulsed laser operation [23].

Fig. 5(a) shows the pulse train of the laser operating at maximum incident pump power of 151.47 mW. The generated stable pulse train is at 67.8 kHz with the full width at half maximum taken as the shortest pulse width of 6.02 μs as shown in the single pulse envelope in Fig. 5(b). Beyond the maximum pump power of 151.47 mW, the Q-switching pulses diminished and can only be recovered by reducing the pump power back to 151.47 mW and below. Hence, no pulse envelop is formed in the output pulse train above the maximum input pump power. Q-switched mode-locking regime which is caused by the large oscillations of the laser's pulse
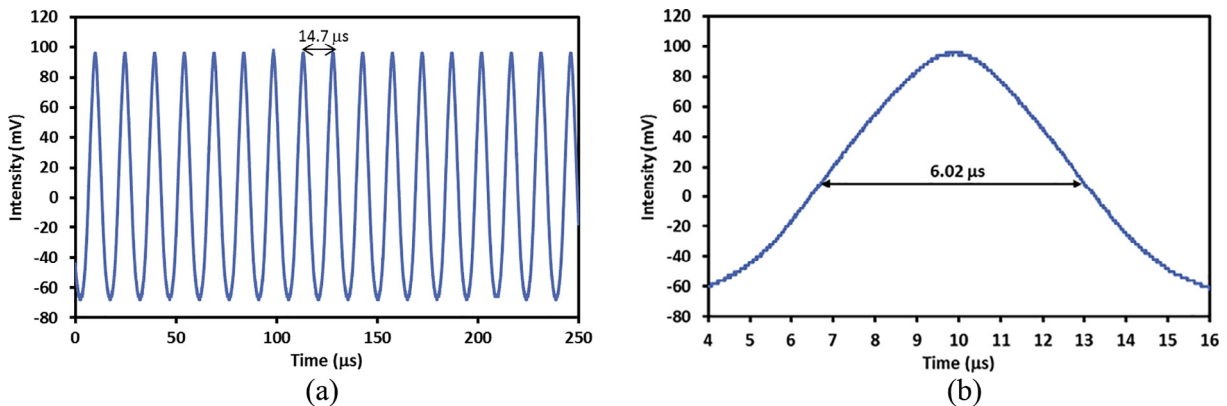

(a)

(b)

Fig. 5. (a) Pulse train of 67.8 kHz at maximum input power (b) Single pulse envelope of the shortest pulse width of 6.02 μs.
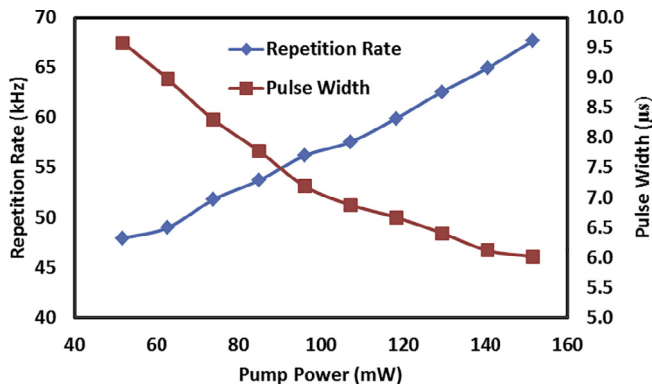
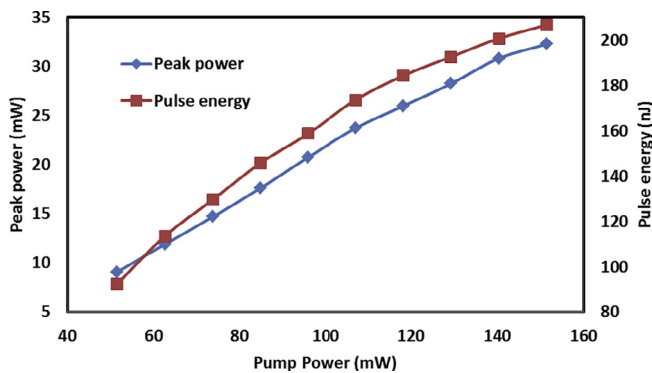**Fig. 6.** Repetition rate and pulse width with respect to input pump powers.

Fig. 7. Instantaneous peak power and pulse energy with respect to input pump powers.
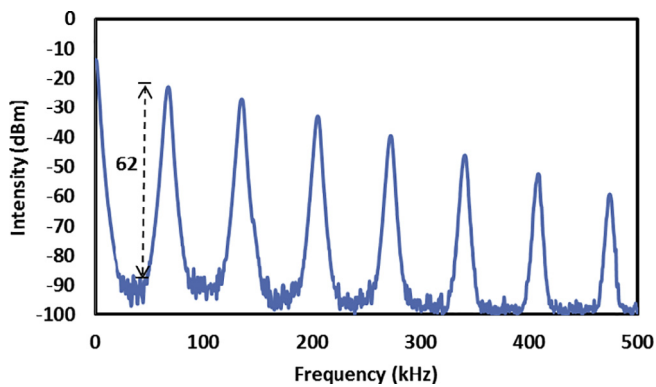

Fig. 8. RFSA measurement signal to noise ratio with first beat note of 62 dB with 500 kHz span.

energy is not observed even at a higher pumping level. This regime is possible if proper alignment and optimization of the laser cavity [24] is done to allow for accurate control of the cavity's parameters [25] in order to assist mode-locking pulses formation.

To further analyze the dependency of the repetition rate and pulse width on the input pump power, the relation of repetition rate and pulse width as function of pump power is illustrated in Fig. 6. The repetition rate increases from 47.94 kHz to 67.8 kHz, almost linearly with the increasing pump power. As the input pump power is increased from 51.6 mW to 151.47 mW, the pulse width is reduced from 9.58 μs to 6.02 μs, indicating inversely proportional trend as can also be seen in other previously reported works [26,27]. From the recorded repetition rate and pulse width,

the instantaneous peak power and pulse energy is calculated and tabulated in Fig. 7. The peak power and pulse energy increases proportionally as the input pump power is tuned from 51.6 mW to 151.47 mW. The maximum peak power and pulse energy recorded is at 32.26 mW and 206.62 nJ, respectively, higher than the reported ones based on 2D material as saturable absorber [16,17,27–30].

The stability of the generated Q-switched pulse, the radio frequency spectrum analyzer (RFSA) is used. The measurement of the RFSA is as plotted in Fig. 8. The first beat node at fundamental repetition rate of 67.8 kHz is about 62 dB, higher than other reported signal-to-noise ratio (SNR) in previous works [19,31] indicating high pulse stability.

Conclusion

The proposed experimental works by using conductive graphene as passive saturable absorber in generating Q-switched pulse laser is successfully demonstrated. This work revealed high generated instantaneous peak power and pulse energy and the performance of the pulse laser is as discussed.

Acknowledgments

References

[1] Ismail M, Ahmad F, Harun S, Arof H, Ahmad H. A Q-switched erbium-doped fiber laser with a graphene saturable absorber. Laser Phys Lett 2013;10 (2):025102.

[2] Woodward RI, Kelleher JR. 2D saturable absorbers for fibre lasers. Appl Sci 2015;5:1440–56.

[3] Lin YH, Yang CY, Liou JH, Yu CP, Lin GR. Using graphene nano-particle embedded in photonic crystal fiber for evanescent wave mode-locking of fiber laser. Opt Express 2013;21(14):16763–75.

[4] Lin GR, Lin YC. Directly Exfoliated and imprinted graphite nano-particle saturable absorber for passive mode-locking erbium-doped fiber laser. Laser Phys Lett 2011;8(12):880–6.

[5] Chiu JC, Lan YF, Chang CM, Chen XZ, Yeh CY, Lee CK, Lin GR, Lin JJ, Cheng WH. Concentration effect of carbon nanotube based saturable absorber on stabilizing and shortening mode-locked pulse. Opt Express 2010;18 (4):3592–600.

[6] Lin YH, Yang CY, Lin SF, Tseng WH, Bao Q, Wu CI, Lin GR. Soliton compression of the erbium-doped fiber laser weakly started mode-locking by nanoscale P-Type Bi₂Te₃ topological insulator particles. Laser Phys Lett 2014;11:055107.

[7] Young R, Deng L, Gong L, Kinloch I. Carbon in polymer. In: Springer Handbook of Nanomaterials. p. 695–728.

[8] Secor EB, Prabhumirashi PL, Puntambekar K, Geier ML, Hersam MC. Inkjet printing of high conductivity, flexible graphene patterns. J Phys Chem Lett 2013;4(8):1347–51.

[9] Dragoman M, Muller AA, Dragoman D, Plana R. Terahertz antenna based on graphene. J Appl Phys 2010;107(10):104313.

[10] Sajal SZ, Bransten BD, Marinov VR. A microstrip patch antenna manufactured with flexible graphene-based conducting material. In: 2015 IEEE International Symposium on Antennas and Propagation & USNC/URSI National Radio Science Meeting. p. 2415–6.

[11] Akbari M, Khan MW, Hasani M, Sydanheimo L, Ukkonen L. Fabrication and characterization of graphene antenna for low-cost and environmentally friendly RFID tags. IEEE Ant Wireless Propagation Lett 2016;15:1569–72.

[12] Tung TT, Chen SJ, Fumeaux C, Losic DS. Scalable realization of conductive graphene films for high-efficiency microwave antennas. J Mater Chem C 2016;4(45):10620–4.

[13] Gomez-Diaz JS, Perruisseau-Carrier J. Microwave to THz properties of graphene and potential antenna applications. In: Proc. of ISAP2012, Oct. 29–Nov. 2, 2012, Nagoya, Japan. p. 239–41.

[14] Perruisseau-Carrier J. Graphene for antenna applications: opportunities and challenges from microwaves to THz. Loughborough Antennas Propag Conf 2012.

[15] Bonaccorso F, Sun Z, Hasan T, Ferrari A. Graphene photonics and optoelectronics. Nat Photonics 2010;4(9):611–22.

[16] Hongwei C, Shengzhi Z, Tao L, Kejian Y, Guiqiu L, Dechun L. Dual-wavelength passively Q-switched Nd, Mg:LiTa$_O$3 laser with a monolayer graphene as saturable absorber. IEEE J Selected Topics Quantum Electron 2015;21 (1):343–7.

[17] Zhao J, Wang Y, Yan P, Ruan S, Cheng J, Du G. Graphene-oxide-based Q-switched fiber laser with stable five-wavelength operation. Chin Phys Lett 2012;29(11):114206.

[18] Sobon G, Sotor J, Jagiello J, Kozinski R, Librant K, Zdrojek M. Linearly polarized, Q-switched Er-doped fiber laser based on reduced graphene oxide saturable absorber. Appl Phys Lett 2012;101(24):241106.

[19] Popa D, Sun Z, Hasan T, Torrisi F, Wang F, Ferrari A. Graphene Q-switched, tunable fiber laser. Appl Phys Lett 2011;98(7):073106.

[20] Boguslawski J, Sotor J, Sobon G, Kozinski R, Librant K, Aksienionek M. Graphene oxide paper as a saturable absorber for Er- and Tm-doped fiber lasers. Photonics Res 2015;3(4):119.

[21] Martinez A, Sun Z. Nanotube and graphene saturable absorbers for fibre lasers. Nat Photonics 2013;7:842–5.

[22] Xin H, Hang Z, Wei L, Rongfei W, Jianrong Q, Mei Z, Bin H. PVP-Assisted solvothermal synthesis of high-yielded Bi2Te3 hexagonal nanoplates: application in passively Q-switched fiber laser. Sci Rep 2015;5:15868.

[23] Sobon G, Sotor J, Przewolka A, Pasternak I, Strupinski W, Abramski K. Amplification of noise-like pulses generated from a graphene-based Tm-doped all-fiber laser. Opt Express 2016;24(18):20359.

[24] Kong LC, Xie GQ, Yuan P, Qian LJ, Wang SX, Yu HH, Zhang HJ. Passive Q-switching and Q-switched mode-locking operations of 2 μm: CLNGG laser with MoS2 saturable absorber mirror. Photon Res 2015;3(2):A47–50.

[25] Keller U, Weingarten KJ, Kartner FX, Kopf D, Braun B, Jung ID, Fluck R, Honninger C, Matuschek N, der Au JA. Semiconductor Saturable Absorber Mirrors (SESAM's) for Femtosecond to nanosecond pulse generation in solid-state lasers. IEEE J Selected Topics Quantum Electron 1996;2(3).

[26] Wang Z, Chen Y, Zhao C, Zhang H, Wen S. Switchable dual-wavelength synchronously Q-switched erbium-doped fiber laser based on graphene saturable absorber. IEEE Photonics J 2012;4(3):869–76.

[27] Saleh Z, Anyi C, Rahman A, Ali N, Harun S, Manaf M. Q-switched erbium-doped fibre laser using graphene-based saturable absorber obtained by mechanical exfoliation. Ukrainian J Phys Opt 2014;15(1):24.

[28] Rashid F, Azzuhri S, Salim M, Shaharuddin R, Ismail M. Using a black phosphorus saturable absorber to generate dual wavelengths in a Q-switched ytterbium-doped fiber laser. Laser Phys Lett 2016;13(8):085102.

[29] Liu L, Zheng Z, Zhao X, Sun S, Bian Y, Su Y. Dual-wavelength passively Q-switched erbium doped fiber laser based on an SWNT saturable absorber. Opti Commun 2013;294:267–70.

[30] Ahmad M, Latiff A, Zakaria Z, Harun S. Q-switched ultrafast TDFL using MWCNTs-SA at 2 μm region. Int J Computer Commun Eng 2014;3(6):446–9.

[31] Ahmad H, Hamdan K, Muhammad F, Harun S, Zulkifli M. Switchable dual-wavelength CNT-based Q-switched using Arrayed Waveguide Gratings (AWG). Appl Phys B 2014;118(2):269–74.